79-FM-32

JSC-16080

DEC 1979

# Analysis of Numerical Stability and Amplification Matrices

## Fourth-Order Runge-Kutta Methods



Mission Planning and Analysis Division

September 1979

NASA

National Aeronautics and Space Administration

**Lyndon B. Johnson Space Center**
Houston, Texas

79-FM-32 JSC-16080

SHUTTLE PROGRAM

# ANALYSIS OF NUMERICAL STABILITY AND AMPLIFICATION MATRICES FOURTH ORDER RUNGE-KUTTA METHODS

By Euel W. Kennedy*
Technology Development Office

Approved: _____
Victor R. Bond
Technology Development Office

Approved: _____
Ronald L. Berry, Chief
Mission Planning and Analysis Division

National Aeronautics and Space Administration

Lyndon B. Johnson Space Center

Houston, Texas

September 1979

*Summer Faculty Fellow, California Polytechnic State University at San Luis Obispo.

ACKNOWLEDGMENT

The author has appreciated the support and encouragement extended to him by the personnel of the Mission Planning and Analysis Division at Johnson Space Center.

CONTENTS

## FIGURES

## 1.0 INTRODUCTION

Numerical stability is an important factor in evaluating the merit of a particular numerical solution. It appears that users of numerical algorithms often assume that if their system of linear, constant coefficient differential equations has eigenvalues with real nonpositive parts, and since the (exact) solutions of initial value problems are stable, it is safe to assume that the numerical solutions are also stable. However, an increasing number of dynamical problems with eigenvalues (multiplicity of two or higher) situated close to the imaginary axis seem to present serious difficulties in regards to their numerical integration. For instance, in the study of orbital mechanics (e.g., the linearized Kustaanheimo-Stiefel elements equations for the unperturbed two-body problem), the differential systems often have imaginary or zero eigenvalues of high multiplicity. Certainly a thorough understanding of the numerical solutions of the linear systems would be required prior to undertaking the difficult study of the stability of numerical solutions of nonlinear systems.

While various texts and papers have addressed the stability regions for Runge-Kutta codes and stable solutions, it seems that the analysis is inadequate for many of the current problems. The heavy dependence on test equations that are scalar or (at best) diagonal systems is a part of the problem. In this paper the emphasis is on systems (excluding two preliminary sections) and illustrations. Theorems and definitions are directed towards systems with eigenvalues

$$\lambda = \rho (\cos \theta + i \sin \theta)$$

where $\rho \geq o$ and $90^o \leq \theta \leq 270^o$

and $i = \sqrt{-1}$

Concepts such as amplification matrices, numerical kernels, stable, and exponentially stable numerical solutions are examined. In section 5.0 the techniques of previous sections are applied to certain systems that have Jordan forms, which are nondiagonal with particular interest in the case of imaginary or zero eigenvalues.

## 2.0 AMPLIFICATION FACTORS

The general four-stage explicit Runge-Kutta method advances one step according to

$$y_{n+1} = y_n + h_n \sum_{i=1}^{4} \omega_i f_i \qquad (1)$$

where

$$f_i = f(t_n + a_i h_n,\ y_n + h_n \sum_{j=1}^{i-1} b_{ij} f_j) \qquad (2)$$

for $i = 1,2,3,4$ and $h_n = t_{n+1} - t_n$. The usual approach of matching Taylor series expansions, Lambert (ref. 1) implies that

$$a_1 = o,\ a_i = \sum_{j=1}^{i-1} b_{ij},\ i = 2,3,4 \qquad (3)$$

and consistency requires that

$$\sum_{i=1}^{4} \omega_i = 1 \qquad (4)$$

Numerical stability for Runge-Kutta schemes considers error propagation for the linear, scalar trial equation

$$\dot{y} = \lambda y \qquad (5)$$

where $\lambda$ can be complex valued. Since $f(t,y) \equiv \lambda y$, substitution in equation (2) gives

$$\begin{aligned} f_1 &= \lambda y_n \\ f_2 &= \lambda y_n \left(1 + \lambda h_n a_2\right) \\ f_3 &= \lambda y_n \left(1 + a_3 (\lambda h_n) + a_2 b_{32} (\lambda h_n)^2\right) \\ f_4 &= \lambda y_n \left(1 + a_4 (\lambda h_n) + (a_2 b_{42} + a_3 b_{43})(\lambda h_n)^2 + a_2 b_{32} b_{43} (\lambda h_n)^3\right) \end{aligned} \qquad (6)$$

where the equation (3) relationship is used. Consequently, evaluation of equation (1) using equation (6) yields

$$y_{n+1} = p(\lambda h_n)\ y_n \qquad (7)$$

where

$$p(\lambda h_n) = 1 + \lambda h_n + \left( \sum_{i=2}^{4} a_i \omega_i \right) (\lambda h_n)^2 + (a_2 b_{32} \omega_3 + a_2 b_{42} \omega_4 + a_3 b_{43} \omega_4)(\lambda h_n)^3 + (a_2 b_{32} b_{43} \omega_4)(\lambda h_n)^4 \quad (8)$$

Equation (4) was used to determine the coefficient of $\lambda h_n$ in equation (8). The scalar polynomial (eq. (8)) is called the amplification factor for the four-stage Runge-Kutta method. If the method is to have fourth order, then

$$y(t_{n+i}) - y_{n+i} = O(h^5) \quad (9)$$

where $y(t_{n+i})$ is the exact solution at $t_{n+i}$ and $y_{n+i}$ is the $(n+i)^{th}$ iterate of the algorithm. Solving equation (5) implies the exact relationship:

$$y(t_{n+1}) = e^{\lambda h_n} y(t_n) \quad (10)$$

where

$$h_n = t_{n+1} - t_n$$

Subtracting equation (7) from equation (10) implies that

$$y(t_{n+1}) - y_{n+1} = e^{\lambda h_n} y(t_n) - p(\lambda h_n)\, y_n \quad (11)$$

But

$$y(t_n) = y_n + O(h^5)$$

and by substitution to $O(h^5)$,

$$y(t_{n+1}) - y_{n+1} = \left(e^{\lambda h_n} - p(\lambda h_n)\right) y_n \quad (12)$$

Since to $O(h^5)$

$$e^{\lambda h_n} = \sum_{i=0}^{4} \frac{(\lambda h_n)^i}{i!}$$

it can be deducted from equation (12) that the error amplification factor is

$$p(\lambda h_n) = \sum_{i=0}^{4} \frac{(\lambda h_n)^i}{i!} \tag{13}$$

provided the Runge-Kutta scheme is to be fourth order. The region of absolute stability in this particular method is the set of all $\lambda h$ for which

$$| p(\lambda h) | < 1 \tag{14}$$

where $h$ is a positive number. That is, the graph of the region (in the complex plane)

$$S = \left\{ \mu : \mu \text{ complex and } \left| \sum_{i=0}^{4} \frac{\mu^i}{i!} \right| < 1 \right\} \tag{15}$$

is the stability region of all fourth-order explicit Runge-Kutta methods (with four stages). Figure 1 shows the graph of $S$.

For general Runge-Kutta methods, the amplification factor $p(\mu)$ is a polynomial in $\mu = \lambda h$, which is a function of the order $q$ and the number of stages $s$ of the method

$$p(\mu) = \sum_{i=0}^{q} \frac{\mu^i}{i!} + \sum_{i=q+1}^{s} \eta_i \mu^i \tag{16}$$

where the $\eta_i$ are functions of the Runge-Kutta parameters. Additional information for $s > q \geq 4$ is given in references 2 (sec. 3.3) and 3.

Suppose that

$$y(t_n) - y_n = \epsilon_n \tag{17}$$

where $\epsilon_n$ denotes the global error at time $t_n$, then from equation (11)

$$y(t_{n+1}) - y_{n+1} = e^{\lambda h_n}\, y(t_n) - p(\lambda h_n)\, y_n$$

or

$$\epsilon_{n+1} = e^{\lambda h_n}\, y(t_n) - p(\lambda h_n)\, [y(t_n) - \epsilon_n],$$

$$\epsilon_{n+1} = p(\lambda h_n)\, \epsilon_n \tag{18}$$

to $O(h^5)$. Equation (18) justifies the term amplification factor, and it is clear that if $| p(\lambda h_n) | \leq 1$, then one-step error control has been achieved.

Remarks. The concept of a numerical stability region is dependent on (a) the method (e.g., Runge-Kutta or linear multistep, implicit or explicit, order, number of stages, etc.), and (b) the nature of the trial equation. Regarding (b), it is important to realize that while the region is independent of eigenvalues per se, the analysis that leads to the amplification factor was very dependent on the type of equation (i.e., eq. (5)).

In the "positive lobes" of the stability region S, the set

$$L \subset S,\ L = \{\, \mu \in S : \mu \text{ complex and } \mathrm{Re}\mu > 0 \,\}$$

where $\mathrm{Re}\mu$ is the real part of the complex number $\mu$, is an anomaly associated with certain Runge-Kutta schemes. This phenomenon occurs here because in the partial series expansion of

$$e^{\lambda h} = e^{\alpha h + i\beta h}$$

where

$$i^2 = -1 \quad \text{and} \quad \lambda = \alpha + i\beta$$

The condition

$$\left| \sum_{j=0}^{4} \frac{(\alpha + i\beta)^j}{j!} \right| = 1$$

can occur (because of crossover terms) with $\alpha > o$ where

$$\left| e^{\alpha h + i\beta h} \right| = 1$$

if and only if $\alpha = o$ (assuming $h > o$). The L is usually deleted from the graph of the stability region S for the following reason: pick any $\mu$ with $Re\mu \leq o$ and consider the one-half line or ray starting at the origin and passing through $\mu$. This ray is divided into two sets, each of which is connected; namely, points of the ray inside S and those exterior to S. Now consider a $\mu$ (near the imaginary axis with $Re\mu > o$) such that its ray passes through L. The set L partitions this ray into two sets but the points of the ray in the unstable regions are disconnected, and in fact, separated by the set L. This unstable region near the origin is what detracts from the applicability of L as part of the stability region. See figure 7 for the plot of $| p(\lambda h) |$ with $\lambda_i = \rho_i$ $(\cos 85^o + i \sin 85^o)$ and $\rho_1 = 2$, $\rho_2 = 5$, and $\rho_3 = 10$. Figure 7 illustrates the nature of L.

## 3.0 SYSTEMS OF EQUATIONS

Equations (1) and (2) of the Runge-Kutta method remain unchanged for systems except that y and f are to be considered as n dimensional vectors. The Runge-Kutta parameters and the step sizes are scalars. The linear trial system is

$$\dot{\underline{y}} = \psi \underline{y} \tag{19}$$

where $\psi$ is an n by n constant, diagonal matrix

$$\psi = \text{diag} \{ \lambda_1, \lambda_2, \ldots, \lambda_n \} \tag{20}$$

where $\underline{y} = (y_1, \ldots, y_n)^T$ and $\lambda_i$ are possibly multiple.

Proceeding as before, the relationship

$$\underline{y}_{m+1} = P(\lambda h_m)\, \underline{y}_m \tag{21}$$

is obtained where $P$ is an $n$ by $n$ diagonal matrix,

$$P(\lambda h_m) = \text{diag}\ \{\ p(\lambda_1 h_m),\ p(\lambda_2 h_m),\ldots,p(\lambda_n h_m)\} \tag{22}$$

The scalar $p(\lambda_i h_m)$ is defined by equation (8) for each $i$. The matrix $P(\lambda h_m) \equiv P(h_m \psi)$ will be referred to as the amplification matrix. The global error (eq. (17)) and error propagation formula (eq. (18)) are as before, except $\underline{\epsilon}_m$ is now an $n$ component vector. The region of absolute stability is unchanged; however, to conclude that the numerical integration proceeds in a stable way, it will be necessary that $h_n$ be selected sufficiently small so that

$$|\ p(\lambda_i h_m)\ | \leq 1, \quad i = 1,\ldots,n$$

## 4.0 NUMERICAL STABILITY

The concept of distance will be significant in this section. The norm $||\ ||$, defined

$$||\ A\ || = \sup_{\underline{x} \neq \underline{0}} \frac{||\ A\underline{x}\ ||}{||\ \underline{x}\ ||}$$

for square matrices $A$, and either

$$||\ \underline{x}\ || = \max_{i=1,\ldots,n} |x_i| \quad \text{or} \quad ||\underline{x}|| = \left(\sum_{i=1}^{n} x_i^2\right)^{1/2}$$

for vectors will be adopted. If $A$ is any square matrix, then it follows from the definition of $||\ A\ ||$ that

$$||\ A\underline{x}\ || \leq ||A||\ ||\underline{x}||, \quad \text{all } \underline{x}$$

Numerical stability is a hybrid concept in that it is both method and equation dependent. In contrast to Lyapunov stability, it would seem unreasonable to expect that a classification of eigenvalues of a linear system would suffice as characteristic (of numerical stability) although such a possibility is not ruled out. What is wanted is a definition of stability for a numerical solution

$$\left(\{\underline{y}_i\}_{i=o}^{N} , \{h_i\}_{i=o}^{N-1}\right)$$

which has resulted from the implementation of a numerical algorithm for an initial value problem

$$\left.\begin{aligned} \dot{\underline{y}} &= \underline{f}(t,\underline{y}) \\ \underline{y}(t_o) &= \underline{y}_o \end{aligned}\right\} \tag{23}$$

The definition should enable the user to classify the given solution on the basis of the behavior of certain nearby numerical solutions using the same steps and the same algorithm. The need to keep the steps invariant is required to avoid confusing stability and convergence. The concept of numerical stability introduced below is global (from a numerical viewpoint); i.e., based on behavior at discrete points in the interval $(t_o,t_f) = \{t:t_o \leq t \leq t_f\}$ where

$$t_f = t_o + \sum_{i=o}^{N-1} h_i$$

and makes use of a "discrete tube." Two basic assumptions are made; first, equation (23) has unique solutions in the region of interest and secondly, roundoff error does not occur (i.e., infinite machine precision).

Definition 1. A numerical solution

$$\left(\{\underline{y}_i\}_{i=o}^{N} , \{h_i\}_{i=o}^{N-1}\right) \tag{24}$$

to an initial value problem (eq. (23)) that is generated by a specific numerical algorithm is exponentially stable if positive numbers $\rho$ and $\delta$, $o < \rho < 1$ exist, such that

$$|| \underline{y}_i - \underline{z}_i || \leq \rho^i || \underline{y}_o - \underline{z}_o || \tag{25}$$

for all numerical solutions

$$\left( \{z_i\}_{i=o}^{N} \ , \ \{h_i\}_{i=o}^{N-1} \right)$$

with

$$|| \underline{y}_o - \underline{z}_o || \leq \delta \tag{26}$$

The numerical solution, equation (24), is stable if $\rho = 1$; i.e.,

$$|| \underline{y}_i - \underline{z}_i || \leq || \underline{y}_o - \underline{z}_o || \ , \ i=1,\ldots,N \tag{27}$$

The solution $\{z_i\}_{i=o}^{N}$ is computed according to the same algorithm as equation (24). Equation (24) will be exponentially unstable if in every $\delta$ neighborhood $\underline{y}_o$ (eq. (26)) there exists a numerical solution $\{z_i\}_{i=o}^{N}$ and $\rho>1$ such that

$$|| \underline{y}_i - \underline{z}_i || > \rho^i || \underline{y}_o - \underline{z}_o || \ , \ i=1,\ldots,N \tag{28}$$

Discussion. The above categories of numerical stability are not mutually exclusive, (i.e., an exponentially stable solution is stable but not necessarily conversely, and there exist numerical solutions that are neither stable nor exponentially unstable). It will often be beneficial to view an initial value $\underline{y}_o$ and step sequence $\{h_i\}_{i=o}^{N-1}$ as given; the implementation of the algorithm results in $\{\underline{y}_i\}_{i=1}^{N}$.

Geometrically the concepts of exponentially stable and unstable are straightforward. Figure 2 illustrates the geometry. A discrete tube is a disconnected set of N+1 disks in $t \times R^n$ that are norm dependent for their geometry and that are centered on $\{\underline{y}_i\}$ at time $t_i = t_o + \sum_{j=o}^{i-1} h_j$. The radii of the disks are identified with the right sides of equations (25) and (27).

If the numerical solution, equation (24), is exponentially stable, then application of the given algorithm to any initial value $\underline{z}_o$ within $\delta$ distance of

$y_o$ will produce a sequence of vectors $\{\underline{z}_i\}_{i=1}^{n}$ such that $\underline{z}_i$ is within $\rho^i \| \underline{y}_o - \underline{z}_o \|$ distance of $\underline{y}_i$; for each $i$, $i=1,\ldots,N$. Figure 2 illustrates this situation if $\| \underline{y}_o - \underline{z}_o \| = \delta$ (i.e., $\underline{z}_o$ actually falls on the circumference of the initial disk) then $\underline{z}_i$ would be in or on the $i^{th}$ disk and $\rho<1$. For stability, all the disks have radii $\| \underline{y}_o - \underline{z}_o \|$; thus $\underline{z}_i$ deviates from $\underline{y}_i$ (for all $i$) by no more than $\underline{z}_o$ from $\underline{y}_o$.

Theorem 1. Consider the initial value problem

$$\dot{\underline{y}} = \psi \underline{y} \ , \ y(t_o) = \underline{y}_o \tag{29}$$

where $\psi = \text{diag}\{\lambda_1,\ldots,\lambda_n\}$ with $\text{Re}\lambda_i \leq o$ , for all $i$.

In addition, assume that

$$\left(\{y_i\}_{i=o}^{N} \ , \ \{h_i\}_{i=o}^{N-1}\right) \tag{24}$$

is a numerical solution of equation (29) generated by some explicit Runge-Kutta algorithm with stability region $S$,

$$S = \{\mu : \mu \text{ complex and } |p(\mu)| < 1\} \tag{30}$$

where $p$ is the amplification factor. Then there exists a number $h^*>o$ such that the numerical solution (eq. (24)) is stable if $h_i \epsilon (o,h^*)$ for all $i$.

Proof. From equation (21),

$$\underline{y}_{m+1} = P(\lambda h_m)\ \underline{y}_m \tag{31}$$

where

$$P(\lambda h_m) = \text{diag}\{p(\lambda_1 h_m),\ldots,p(\lambda_n h_m)\}$$

for all m, m=o,1,...,N-1. The symbol $P(\lambda h_m)$ is written as $P(h_m\psi)$ where the $p(\lambda_i h_m)$ are defined in equation (8) for the general, fourth-order Runge-Kutta method and by similar amplification factors in general. Repeated iterations of equation (31) with m=0,1,2,... implies that for any i, i=o,1,...,N-1:

$$\underline{y}_i = \left(P(h_{i-1}\,\psi)\; P(h_{i-2}\,\psi)\ldots P(h_o\,\psi)\right)\underline{y}_o \tag{32}$$

Equation (32), which shows how a solution propagates, can be written (using the $\pi$ product) as

$$\underline{y}_i = \left(\prod_{j=0}^{i-1} P(h_j\,\psi)\right)\underline{y}_o \tag{33}$$

and as a consequence of the diagonal nature of the amplification matrices,

$$\prod_{j=0}^{i-1} P(h_j\,\psi) = \operatorname{diag}\left\{\prod_{j=o}^{i-1} p(\lambda_1 h_j),\ldots,\prod_{j=o}^{i-1} p(\lambda_n h_j)\right\} \tag{34}$$

Similarly, for a numerical solution with initial value $\underline{z}_o$, it is concluded that

$$\underline{z}_i = \left(\prod_{j=o}^{i-1} P(h_j\,\psi)\right)\underline{z}_o \tag{35}$$

The matrix in equation (35) (i.e., the $\pi$ product) will be called the numerical kernel. Subtracting equation (35) from equation (33) and taking norms implies that

$$\|\,\underline{y}_i - \underline{z}_i\,\| = \|\left(\prod_{j=0}^{i-1} P(h_j\,\psi)\right)(\underline{y}_o - \underline{z}_o)\| \tag{36}$$

The $k^{th}$ component of the vector

$$\left(\prod_{j=o}^{i-1} P(h_j\,\psi)\right)(\underline{y}_o - \underline{z}_o) \quad \text{equals} \quad \left(\prod_{j=o}^{i-1} p(h_j\lambda_k)\right)(y_{ko} - z_{ko})$$

where $y_{ko}$ and $z_{ko}$ are the $k^{th}$ components of $\underline{y}_o$ and $\underline{z}_o$. Thus,

$$\left|\left|\left(\prod_{j=o}^{i-1} P(h_j\ \psi)\right)(\underline{y}_o - \underline{z}_o)\right|\right| = \left(\sum_{k=1}^{n}\left(\prod_{j=o}^{i-1} p^2(h_j\lambda_k)\right)(y_{ko} - z_{ko})^2\right)^{1/2}$$

or

$$\left|\left|\left(\prod_{j=o}^{i-1} P(h_j\ \psi)\right)(\underline{y}_o - \underline{z}_o)\right|\right| = \left(\max_k \prod_{j=o}^{i-1} \left| p(k_j\lambda_k) \right|\right) \left| y_{ko} - z_{ko} \right| \quad (37)$$

depending on which norm is used.

Now $Re\lambda_k \leq o$, $k=1,\ldots,n$; thus, there exists $h_k^* > o$ such that $|p(\lambda_k h_k^*)| = 1$, for each $k$ and for all $h$ in the closed interval $o \leq h \leq h_k^*$. It follows that

$$|p(\lambda_k h)| \leq 1$$

Set

$$h^* = \min_k h_k^*\ , \quad (h^* \text{ is positive}) \quad (38)$$

Then if the sequence $\{h_j\}_{j=o}^{N-1}$ has the property that $h_j \varepsilon (o, h^*)$, for all $j$, it is concluded that $|p(h_j\lambda_k)| \leq 1$ for all $j$ and $k$, and consequently,

$$\left(\sum_{k=1}^{n}\left(\prod_{j=o}^{i-1} p^2(h_j\lambda_k)\right)(y_{ko} - z_{ko})^2\right)^{1/2} \leq ||\ \underline{y}_o - \underline{z}_o\ ||$$

and

$$\max_k \left( \prod_{j=o}^{i-1} | p(h_j \lambda_k) | \right) | y_{ko} - z_{ko} | \leq || \underline{y}_o - \underline{z}_o ||$$

Equations (37) then give the necessary conclusion of stability of the numerical equation (24).

Since amplification factors and matrices have dominant roles in the study of numerical stability, it is of value to examine their graphs in detail.

## 4.1 AMPLIFICATION FACTOR GEOMETRY

Graphs of the region of stability (e.g., fig. 1) are too coarse for the present analysis. This section will consider only a four-stage, fourth-order explicit Runge-Kutta method.

In this case,

$$p(h\lambda) = \sum_{j=o}^{4} \frac{(h\lambda)^j}{j!}$$

where $\lambda$ is complex. In polar coordinates,

$$\lambda = \rho(\cos\theta + i \sin\theta)$$

and

$$p(h\lambda) = \sum_{j=o}^{4} \frac{(h\rho(\cos\theta + i \sin\theta))^j}{j!} \tag{39}$$

or

$$p(h\lambda) = \sum_{j=o}^{4} \frac{(h\rho)^j}{j!} (\cos(j\theta) + i \sin(j\theta)) \tag{40}$$

where equation (40) resulted from applying De Moivre's theorem to equation (39). Thus,

$$|p(h\lambda)| = \left[\left(\sum_{j=0}^{4} \frac{(h\rho)^j}{j!}\cos(j\theta)\right)^2 + \left(\sum_{j=0}^{4} \frac{(h\rho)^j}{j!}\sin(j\theta)\right)^2\right]^{1/2} \qquad (41)$$

The first point of view will be to specify various choices of $\lambda$ and plot $|p(h\lambda)|$ as a function of $h$, $h \geq o$. Figures 3 through 7 each consists of three plots of $|p(h\lambda)|$ with the angle $\theta$ fixed, but with $\rho = 2,5$, and 10. Thus, each figure represents the evolution of the graph of $|p(h\lambda)|$ as the modulus $\rho$ of $\lambda$ increases from 2 to 10 (for a fixed angle). However, by fixing $\rho$ (e.g., $\rho=2$) and selecting the corresponding plot in each figure, it can be seen that evolution of $|p(h\lambda)|$ as $\theta$ decreases through the range of $180^o$ (fig. 3), $120^o$ (fig. 4), $90^o$ (fig. 5), and $85^o$ (fig. 7). Figure 6 ($\lambda=o$) is included because it clearly represents a limiting case of the purely imaginary situation (fig. 5); i.e.,

$$|p(o)| = \lim_{\rho \to o} |p(i\rho h)|$$

This indicates that, from the numerical stability view, the behavior of problems with $\lambda=o$ (as in ref. 4) is more closely related to problems with small, purely imaginary eigenvalues than with small, real negative eigenvalues. The concave-downward segment of the graphs for the purely imaginary case ($\theta = 90^o$) suggests that small perturbations could produce either stability or instability if the step sequence were confined to certain intervals (i.e., if $\lambda=2i$, then $h_i \in (0,0.5)$).

Additional global information about the stability region $S$ can be obtained by setting $\mu = h\lambda$ in equation (41) and finding contour lines

$$| p(\mu) | = r, \quad o \leq r \leq 1$$

Figure 8 illustrates the level curve configuration for the fourth-order Runge-Kutta methods, with $r=0.1\,k$, $k=1,2,\ldots,9$. To obtain both quadrants, reflect figure 8 across the negative real axis.

## 4.2 NUMERICAL KERNELS

While theorem 1 applies only to diagonal systems (eq. (29)), it is possible to bring more general systems under that theorem's sphere of influence. Consider a system

$$\dot{\underline{x}} = A\underline{x} \qquad (42)$$

where A is an n by n matrix and such that A is diagonalizable. Thus, there exists a nonsingular matrix M, and

$$M^{-1} AM = \psi_M \tag{43}$$

where $\psi_M$ is diagonal. If the eigenvalues of A are $\{\lambda_i\}_{i=1}^{n}$, then it is well known that

$$\psi_M = \text{diag } \{\lambda_1,\ldots,\lambda_n\} \tag{44}$$

(i.e., eigenvalues are invariant under a similarity transformation).

Remark. The order of the eigenvalues in $\psi_M$ is dependent on M.

Amplification matrices and numerical kernels for equation (42) is now considered. In fact, the development in equations (1) through (8) extends naturally to vector systems. Thus, if

$$f(\underline{x}) = A\underline{x} \tag{45}$$

then equations (6) become

$$\underline{f}_1 = A\underline{x}_n$$

$$\underline{f}_2 = A\left(I + a_2 (h_nA)\right) \underline{x}_n$$

$$\underline{f}_3 = A\left(I + a_3 (h_nA) + a_2b_{32} (h_nA)^2\right) \underline{x}_n$$

$$\underline{f}_4 = A\left(I + a_4 (h_nA) + (a_2b_{42} + a_3b_{43}) (h_nA)^2 + a_2b_{32}b_{43} (h_nA)^3\right) \underline{x}_n$$

where I is the n by n identity matrix and

$$\underline{x}_{n+1} = P(h_nA)\underline{x}_n \tag{46}$$

where

$$P(h_nA) = I + h_nA + \left(\sum_{i=2}^{4} a_i\omega_i\right)(h\,A)^2 + (a\,b\;\omega_3 + a_2b_{42}\omega_4 + a_3b_{43}\omega_4)\,(h_nA)^3 + (a_2b_{32}b_{43}\omega_4)\,(h_nA)^4 \tag{47}$$

Further, to $O(h_n^5)$,

$$e^{h_nA} = \sum_{j=0}^{4} \frac{(h_nA)^j}{j!}$$

which implies that the matrix analog of equation (13) is namely

$$P(h_nA) = \sum_{j=0}^{4} \frac{(h_nA)^j}{j!} \tag{48}$$

If the view is taken that a step-size sequence $\{h_i\}_{i=0}^{N-1}$ is given, then at any time $t_i$, $t_i = t_o + \sum_{j=0}^{i-1} h_j$, the $i^{th}$ iterate $\underline{x}_i$ is defined recursively by formula equation (46) or

$$\underline{x}_i = P(h_{i-1}A)\,P(h_{i-2}A)\ldots P(h_oA)\,\underline{x}_o \tag{49}$$

or

$$\underline{x}_i = \left(\prod_{j=0}^{i-1} P(h_jA)\right)\underline{x}_o \tag{50}$$

where it is understood that the $\pi$ product in equation (49) is ordered as in equation (49). The amplification matrices in equation (49) are not commutative. The $\pi$ product in equation (50) is called the numerical kernel (associated with the $i^{th}$ iterate). An important relationship is now established.

Observation 1. Amplification factors (for Runge-Kutta methods) are invariant under similarity transformation (i.e., if $A$ is similar to $\psi_M$, then $P(h_nA)$ is similar to $P(h_n\psi_M)$).

Proof. First,

$$A^i = AM(M^{-1} AM)^{i-2} M^{-1} A, \text{ for } i \geq 2 \tag{51}$$

but

$$P(h_n A) = \sum_{i=o}^{4} \frac{(h_n A)^i}{i!} \tag{52}$$

and consequently,

$$M^{-1} P(h_n A)M = \sum_{i=o}^{4} \frac{h_n{}^i (M^{-1} AM)^i}{i!}$$

$$= \sum_{i=o}^{4} \frac{(h_n \psi_M)^i}{i!}$$

$$= P(h_n \psi_M) \tag{53}$$

This completes the proof.

It should be observed that the subscript of $\psi_M$ is necessary in the sense that while the diagonal elements of $\psi_M$ are exactly $\{\lambda_1,\ldots,\lambda_n\}$, the order may not be preserved; i.e., $\psi_M = \text{diag}\ \{\lambda_{i1},\lambda_{i2},\ldots,\lambda_{in}\}$ where the two eigenvalue sets are equal in elements and multiplicities.

The previous result is extented to numerical kernels.

Observation 2. Numerical kernels for Runge-Kutta methods are invariant under similarity transformation (i.e., if A is similar to $\psi_M$, then K (A) is similar to $K_i(\psi_M)$).

Proof. From equation (50), the numerical kernel for equation (42) is

$$K_i(A) = \prod_{j=o}^{i-1} P(h_j A) \tag{54}$$

Hence,

$$M^{-1} K_i(A)M = \prod_{j=o}^{i-1} \left(M^{-1}P(h_jA)M\right)$$

$$= \prod_{j=o}^{i-1} P(h_j\psi_M) = K_i(\psi_M) \qquad (55)$$

Observe that the numerical kernel for $\psi_M$ is diagonal. Equation (54) introduces the notation $K_i$ for the kernel; thus, the $i^{th}$ iterate of a numerical solution starting at $x_o$ with step sequence $\{h_i\}_{i=o}^{N-1}$ is

$$\underline{x}_i = K_i(A)\underline{x}_o, \; i=1,2,\ldots,N \qquad (56)$$

Equation (56) generates a numerical approximation to

$$\dot{\underline{x}} = A\underline{x} \; , \; \underline{x}\,(t_o) = \underline{x}_o$$

By multiplying equation (56) by $M^{-1}$ on the right, it follows that

$$M^{-1}\underline{x}_i = M^{-1} K_i(A) \; \underline{x}_o$$

$$= M^{-1} K_i(A) \; M(M^{-1} \; \underline{x}_o)$$

or

$$M^{-1}\underline{x}_i = \left(K_i(\psi_M)\right) \; (M^{-1} \; \underline{x}_o) \qquad (57)$$

where observation 2 was used to obtain equation (57).

If

$$\underline{y}_o = M^{-1}\underline{x}_o$$

is set in equation (57), then that equation generates an approximate solution to the initial value problem

$$\dot{\underline{y}} = \Psi_M \underline{y} \quad , \; y(t_o) = \underline{y}_o$$

Multiplication of equation (57) by $M$ (on the left) gives

$$\underline{x}_i = \left(M \, K_i(\Psi_M) \, M^{-1}\right) \underline{x}_o \tag{58}$$

It should be noted that $K_i(\Psi_M)$ and $K_i(A)$ are step sequence dependent; i.e., functions of $\{h_j\}_{j=o}^{N-1}$.

## 4.3 STABILITY BOUNDS

Theorem 2. Consider the initial value problem

$$\dot{\underline{y}} = \Psi \underline{y} \quad , \quad \underline{y}\,(t_o) = \underline{y}_o \tag{59}$$

where $\Psi = \text{diag}\,\{\lambda_1,\ldots,\lambda_n\}$ with $\text{Re}\,\lambda_i \leq o$ for all $i$. Let

$$\left(\{y_i\}_{i=o}^{N} \; , \; \{h_i\}_{i=o}^{N-1}\right)$$

be a numerical solution of equation (59) generated by an explicit Runge-Kutta algorithm. Then there exists symbols $\rho_k$, $\tau_k$ and an interval $(h_L,h_R)$ such that $o < \rho_k \leq 1$ and $o < \tau_k \leq 1$, and if $h_i \in (h_L,h_R)$ for all $i$, then the $k^{th}$ component of $\underline{y}_i$, namely $y_{ki}$, satisfies the inequality.

$$\tau_k^i \, | \, y_{ko} - z_{ko} \, | \leq | \, y_{ki} - z_{ki} \, | \leq \rho_k^i \, | \, y_{ko} - z_{ko} \, | \tag{60}$$

for all $i$, $i=1,2,\ldots,N$ and all $k$, $k=1,\ldots,n$. The inequalities in equation (60), $\left(\{\underline{z}_i\}_{i=o}^{N} \; , \; \{h_i\}_{i=o}^{N-1}\right)$ is any other numerical solution.

Proof. For each $\lambda_k$, there exists $h_k^* > o$ such that

$$| \, p(\lambda_k \, h_k^*) \, | = 1$$

and for all $h$, $o \leq h \leq h_k^*$

$$| p(\lambda_k h) | \leq 1$$

Set

$$h^* = \min_k \{h_k^*\}$$

and suppose

$$(h_L, h_R) \subset (o, \cdot\cdot)$$

where

$$h_L = \min_i \{h_i\}, \quad h_R = \max_i \{h_i\}$$

Since

$$f_k(h) = | p(\lambda_k h) |$$

is a continuous function and $(h_L, h_R)$ is a compact set, there exists positive symbols $\tau_k$ and $\rho_k$ such that

$$\min_{h\varepsilon(h_L,h_R)} | p(\lambda_k h) | \equiv \tau_k \leq | p(\lambda_k h) | \leq \rho_k \equiv \max_{h\varepsilon(h_L,h_R)} | p(\lambda_k h) | \qquad (61)$$

where the inequalities in equation (61) hold for all $h\varepsilon(h_L, h_R)$.

Now

$$\underline{Y}_i = \left( \prod_{j=o}^{i-1} P(h_j \psi) \right) \underline{Y}_o$$

which implies that

$$y_{ki} = \left( \prod_{j=o}^{i-1} p(\lambda_k h_j) \right) y_{ko} \tag{62}$$

and

$$z_{ki} = \prod_{j=o}^{i-1} p(\lambda_k h_j)\, z_{ko} \tag{63}$$

Subtracting equation (63) from equation (62), and taking absolute values

$$| y_{ki} - z_{ki} | = \left( \prod_{j=o}^{i-1} | p(\lambda_k h_j) | \right) | y_{ko} - z_{ko} | \tag{64}$$

but

$$\prod_{j=o}^{i-1} \tau_k \leq \prod_{j=o}^{i-1} | p(\lambda_k h_j) | \leq \prod_{j=o}^{i-1} \rho_k$$

or

$$\tau_k^i \leq \prod_{j=o}^{i-1} | p(\lambda_k h_j) | \leq \rho_k^i$$

which, with equation (64) implies that the conclusion for each $i$ and $k$.

Discussion. The interval $(h_L, h_R)$ is referred to as the step interval for a particular numerical solution. Since $| p(\lambda_k h) | = | p(\bar{\lambda}_k h) |$, then if conjugate pairs of complex eigenvalues occur, it is only necessary to compute $\tau_k$ and $\rho_k$ for one of the pair. Figure 9 illustrates the theorem for equation (59) with eigenvalues $\{ \pm 5i, -2, 5(\cos 120^\circ + i \sin 120^\circ) \}$. Clearly, the bounds would be sharper if step variations were small; that is, $h_R - h_L$ were near zero.

## 5.0 ERROR PROPAGATION FOR NONDIAGONAL SYSTEMS

From the study of Lyapunov stability (ref. 5), it is well known that if a linear, constant coefficient differential system

$$\dot{\underline{x}} = A\underline{x}$$

has eigenvalues $\{(\lambda i)_{i=1}^{n}\}$ and Re $\lambda i < 0$ for all $i$, then the solutions are stable (in fact, asymptotically stable), and this is the case even if there are multiple eigenvalues. An analogous question in numerical stability would be the following: Consider two constant coefficient, linear systems of equal dimension:

$$\dot{\underline{x}} = A_1 x \ , \quad \dot{\underline{x}} = A_2 \underline{x}$$

in which the Jordan canonical form of $A_1$ and $A_2$ are given by:

$$M_1^{-1} A_1 M_1 = J_1 \ , \quad M_2^{-1} A_2 M_2 = J_2$$

and the eigenvalues of $J_1$ and $J_2$ are identical in form and multiplicity but $J_1$ is diagonal and $J_2$ is not. Thus,

$$J_1 = \text{diag}\ (\lambda_1,\ldots,\lambda_1;\ \lambda_2,\ldots,\lambda_2;\ldots;\lambda_r,\ldots,\lambda_r)$$

where

$$\sum_{i=1}^{r} \text{multiplicities of } \lambda_i = n,$$

and

$$J_2 = \text{diag}\ \{A_1, A_2, \text{---}, A_r\}$$

where $A_i$ is a square matrix with dimension equal to the multiplicity of $\lambda_i$, and (ref.6)

$$A_i = \begin{pmatrix} \lambda_i & \delta i_1 & o & \cdots & o \\ o & \lambda_i & \delta i_2 & o & \cdots & o \\ o & \cdots & \lambda_i & \delta i_k & & \\ o & \cdots & o & \lambda_i & & \end{pmatrix}, \quad \delta_{ij} = o \text{ or } 1$$

Then, as has been proven in theorem 1, if $\text{Re}\ \lambda_i \leq 0$, the numerical solutions of

$$\dot{\underline{y}} = J_1 \underline{y}$$

where $\underline{y} = M_1^{-1} \underline{x}$ are stable provided the step sequence $\{h_i\}_{i=1}^{N-1}$ is admissible in the sense of the statement of the theorem. What then can be said for the stability of the solutions of

$$\dot{\underline{y}} = J_2 \underline{y}$$

Since the test algorithm is fourth order Runge-Kutta, a related question concerns the relationship, if any, between the contour curves for $|p(\mu)|$ (fig. 8) and error propagation (i.e., does the topography of $|p(\mu)|$ influence error propagation?), figure 8 has several distinct features including two wells and a "plateau" centered on the imaginary axis and extending out about 1.5 units.

Specifically considered are examples having the general form

$$J_2 = \begin{pmatrix} \lambda_1 & \delta_1 & o & o \\ o & \lambda_1 & \delta_2 & o \\ o & o & \bar{\lambda}_1 & \delta_3 \\ o & o & o & \bar{\lambda}_1 \end{pmatrix} \tag{65}$$

where $\bar{\lambda}_1$ is the complex conjugate of $\lambda_1$. Equation (65) can include complex eigenvalues of multiplicity two (e.g., $\lambda_1 = i$, $\bar{\lambda}_1 = -i$ where $i^2 = -1$) and nonpositive real roots of multiplicity four. These cases are of particular interest in orbital motion equations and mechanical systems. The amplification matrix associated with equation (65) is

$$P(h J_2) = \sum_{j=0}^{4} \frac{(hJ_2)^j}{j!} \tag{66}$$

and the error vector $\underline{\varepsilon}_m$ propagates according to

$$\underline{\varepsilon}_{m+1} = P(hJ_2)\, \underline{\varepsilon}_m$$

where

$$\underline{\varepsilon}_m = (\varepsilon_1^m, \ldots, \varepsilon_n^m)^T \tag{67}$$

and a constant step size $h$ is assumed. The amplification matrix $P(hJ_2)$ is given by

$$P(h J_2) = \begin{pmatrix} p(h\lambda_1) & p_{12} & p_{13} & p_{14} \\ o & p(h\lambda_1) & p_{23} & p_{24} \\ o & o & p(h\bar{\lambda}_1) & p_{34} \\ o & o & o & p(h\bar{\lambda}_1) \end{pmatrix} \tag{68}$$

where $p(h\lambda)$ is defined in equation (13),

$$p_{12} = h\,\delta_1 \left(1 + h\,\lambda_1 + \frac{(h\,\lambda_1)^2}{2!} + \frac{(h\,\lambda_1)^3}{3!}\right)$$

$$p_{23} = h\,\delta_2 \left(1 + \frac{h(\lambda_1 + \bar{\lambda}_1)}{2!} + \frac{h^2(\lambda_1^2 + \lambda_1\bar{\lambda}_1 + \bar{\lambda}_1^2)}{3!} + \frac{h^3(\lambda_1^3 + \lambda_1^2\,\bar{\lambda}_1 + \lambda_1\bar{\lambda}_1^2 + \bar{\lambda}_1^3)}{4!}\right)$$

$$p_{34} = h\,\delta_3 \left(1 + h\,\bar{\lambda}_1 + \frac{(h\bar{\lambda}_1)^2}{2!} + \frac{(h\bar{\lambda}_1)^3}{3!}\right)$$

$$p_{13} = h^2\,\delta_1\delta_2 \left(\frac{1}{2!} + \frac{h\,(2\lambda_1 + \bar{\lambda}_1)}{3!} + \frac{h^2(3\lambda_1^2 + 2\,\lambda_1\bar{\lambda}_1 + \bar{\lambda}_1^2)}{4!}\right)$$

and

$$p_{14} = h^3 \delta_1\delta_2\delta_3 \left(\frac{1}{3!} + \frac{h\,(2\lambda_1 + 2\bar{\lambda}_1)}{4!}\right)$$

In the study of error propagation, the equations to be considered are:

$$\begin{aligned}
\epsilon_1^{m+1} &= p(h\lambda_1)\,\epsilon_1^m + p_{12}\,\epsilon_2^m + p_{13}\,\epsilon_3^m + p_{14}\,\epsilon_4^m \\
\epsilon_2^{m+1} &= p(h\lambda_1)\,\epsilon_2^m + p_{23}\,\epsilon_3^m + p_{24}\,\epsilon_4^m \\
\epsilon_3^{m+1} &= p(h\bar{\lambda}_1)\,\epsilon_3^m + p_{34}\,\epsilon_4^m \\
\epsilon_4^{m+1} &= p(h\bar{\lambda}_1)\,\epsilon_4^m
\end{aligned} \tag{69}$$

It will be assumed that control of error propagation has occurred if for any vector $\underline{\epsilon}^0 = (\epsilon_1^0, \epsilon_2^0, \epsilon_3^0, \epsilon_4^0)^T$ with components $|\epsilon_i^0| \leq 1$, it follows that the components $\epsilon_i^{m+1}$ of $\underline{\epsilon}^{m+1}$ (defined iteratively by equation (69)) satisfy

$$|\epsilon_i^{m+1}| \leq 1 \tag{70}$$

for all $i$ and $m$.

This can be phrased as: all components of the error vector iterates are within the unit disk if the initial error has components within that disk.

In this document, the analysis is restricted to equation (65) with $\delta_1 = 1$, $\delta_2 = 0$ and $\delta_3 = 0$. An examination of $p_{ij}$ factors shows that $p_{ij} = 0$ except for $i = 1$ and $j = 2$ and in this case,

$$\begin{aligned}
p_{12} &= h\left(1 + h\lambda_1 + \frac{(h\lambda_1)^2}{2!} + \frac{(h\lambda_1)^3}{3!}\right) \\
&= \frac{1}{\lambda_1}\left(h\lambda_1 + (h\lambda_1)^2 + \frac{(h\lambda_1)^3}{2!} + \frac{(h\lambda_1)^4}{3!}\right), \text{ if } \lambda_1 \neq 0
\end{aligned} \tag{71}$$

Note that

$$\lim_{|\lambda_1| \to o} |p_{12}| = h$$

That is, the graph of $|p_{12}|$ (as a function of h) approaches the $45^o$ line as $|\lambda_1| \to o$.

Equations (69) reduce to

$$\begin{aligned} \epsilon_1^{m+1} &= p(h\lambda_1)\, \epsilon_1^m + p_{12}\, \epsilon_2^m \\ \epsilon_j^{m+1} &= p(h\lambda)\, \epsilon_j^m, \quad j = 2,3,4 \text{ and } \lambda = \lambda_1 \text{ or } \bar{\lambda}_1 \end{aligned} \tag{72}$$

In contrast to our previous study of amplification factors for diagonal matrices, the factor $\epsilon_1^{m+1}$ is propagated as coupled function of $\epsilon_1^m$ and $\epsilon_2^m$, the amplification factor $p_{12}$ is a function of the eigenvalue $\lambda$ and finally, the triangle inequality is too coarse to use in the analysis; i.e.,

$$\begin{aligned} |\epsilon_1^{m+1}| &= | p(h\lambda_1)\, \epsilon_1^m + p_{12}\, \epsilon_2^m | \\ &\leq | p(h\lambda_1) |\, | \epsilon_1^m | + | p_{12} |\, | \epsilon_2^m | \end{aligned}$$

does not admit the type of conclusions desired. Certain conclusions do seem justifiable for eigenvalues of the form $i\beta$, $\beta \geq o$ from an analysis of $|p_{12}|$, especially when coupled with the previous work on $|p(h\lambda)|$. Figures 10 and 11 give the plots of $|p_{12}|$ for $\lambda = \rho(\cos\theta + i \sin\theta)$, with $\rho=2$, and for selected values of $\theta$. When the graph of $|p_{12}|$ for $\theta = 90^o$ (i.e., $\lambda_1=2i$) in figure 10 is compared with the graph of $|p(\lambda h)|$ in figure 3, it is apparent that error propagation will not be controlled. This observation also holds for $\lambda=o$; e.g., zero is eigenvalue of multiplicity four but with nondiagonal Jordan form.

It should be realized that it is unnecessary to be concerned with $\epsilon_j^{m+1}$, $j \geq 2$ since we have assumed that $h\lambda$ is within the stability region S, and consequently

$$| \epsilon_j^{m+1} | \leq | \epsilon_j^m |, \quad j = 2,3,4$$

Preliminary work has indicated that for certain initial errors ($\epsilon_j^0 = 1$, $j = 1,2,3,4$) there are regions in the second quadrant for which the first iteration fails to satisfy inequalities in equation (70); i.e.,

$$| \epsilon_1^1 | > | \epsilon_1^0 | = 1$$

Figure 12 illustrates the situation for $\lambda = 2(\cos\theta + i \sin\theta)$, and the polar coordinate distance is $\rho h = 2h$.

A comparison of figures 8 and 12 suggests that the plateau centered on the imaginary axis had significant influence on the plot of $| \epsilon_1^1 |$. It has also been observed that if iterations of $\underline{\epsilon}^0$ are continued according to equation (72) then equation (70) may be met for sufficiently large m, even if operating in the area between the imaginary axis and the boundary of $| \epsilon_1^1 | \leq 1$.

## 6.0 CONCLUSIONS

The plots of stability regions alone are inadequate to study stability or error propagation of numerical solutions that correspond to linear systems having repeated complex roots, and the problem is more acute for eigenvalues near the imaginary axis; i.e., with angles slightly larger than 90°. There is increasing evidence that most numerical integrators such as explicit Runge-Kutta and linear multistep methods have difficulty with such differential systems and improvement of the performance of the algorithms will depend on the recognition of what causes the problem. It is suggested in this paper that more emphasis must be placed on error propagation in the case that Jordan Canonical form of the A matrix is nondiagonal. That is, where the system is $\dot{\underline{x}} = A\underline{x}$. In fact, a lack of understanding of exactly what numerical stability is or should be is a large part of the problem. In this paper, various definitions are put forth for numerical stability, and the amplification matrix is studied in detail (for the fourth-order Runge-Kutta method) in order to understand reasons for the apparent failure of stability in the situations given in this paper. For the case in which the A matrix is diagonalizable, a fairly complete theory exists and several theorems are proven for that case. Theorems on the existence of numerical stability and stability bounds are also presented.

Evidence that a plateau, centered on the imaginary axis and extending out from the origin, may have sufficient influence to cause instability for repeated eigenvalues when arguments $\theta$, $90° \leq \theta < 120°$ are given. It is also noted that (from the numerical stability viewpoint) an eigenvalue of zero should be considered as a limiting case of $i\beta$ where $i^2 = -1$ and $\beta \to 0$ rather than as a negative real number (tending to zero). It is clear that additional studies are required with computer support, but the preliminary analyses by the techniques of this paper appear to have potential.

## 7.0 REFERENCES

1. Lambert, J. D.: Computational Methods in Ordinary Differential Equations. John Wiley and Sons, Inc., 1973.

2. Shampine, L.; and Watts, H.: Practical Solution of Ordinary Differential Equations by Runge-Kutta Methods. Sandia Laboratories Report SAND 76-0585, Dec. 1976.

3. Watts, Herman A.: Runge-Kutta-Fehlberg Methods: Scaled Stability Regions. Sandia Laboratories Report SAND 76-0323, July 1976.

4. Bond, V. R.; and Horn, M. K.: Error Propagation in Orbital Motion Equations using Runge-Kutta Methods. NASA TM X-58216.

5. Kennedy, E. W.: Lyapunov Stability and its Application to Systems of Ordinary Differential Equations. JSC IN 79-FM-31, Sept. 1979.

6. Finkbeiner, Daniel T.: Introduction to Matrices and Linear Transformations. W. H. Freeman and Co., 1960.

7. Gear, C. William: Numerical Initial Value Problems in Ordinary Differential Equations. Prentice Hall, Inc., 1971.

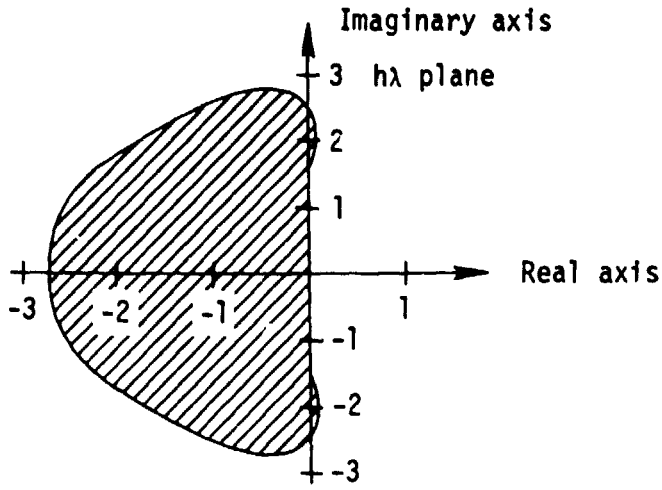


Figure 1.- Region of absolute stability of fourth-order explicit Runge-Kutta method (ref. 7,p.41).

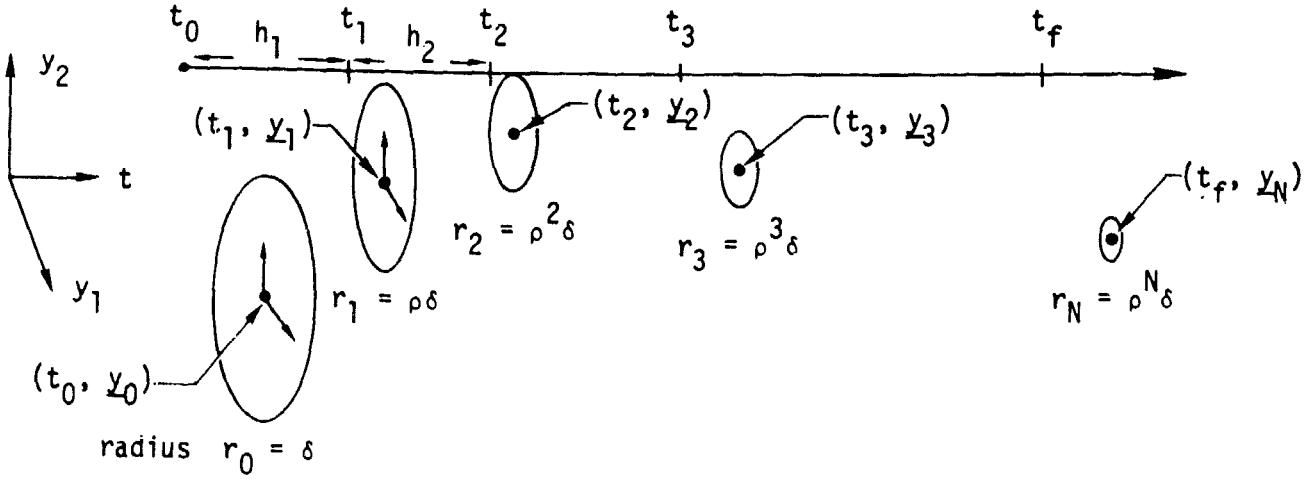


Figure 2.- A "discrete tube" $t \times R^2$ associated with a numerical solution.

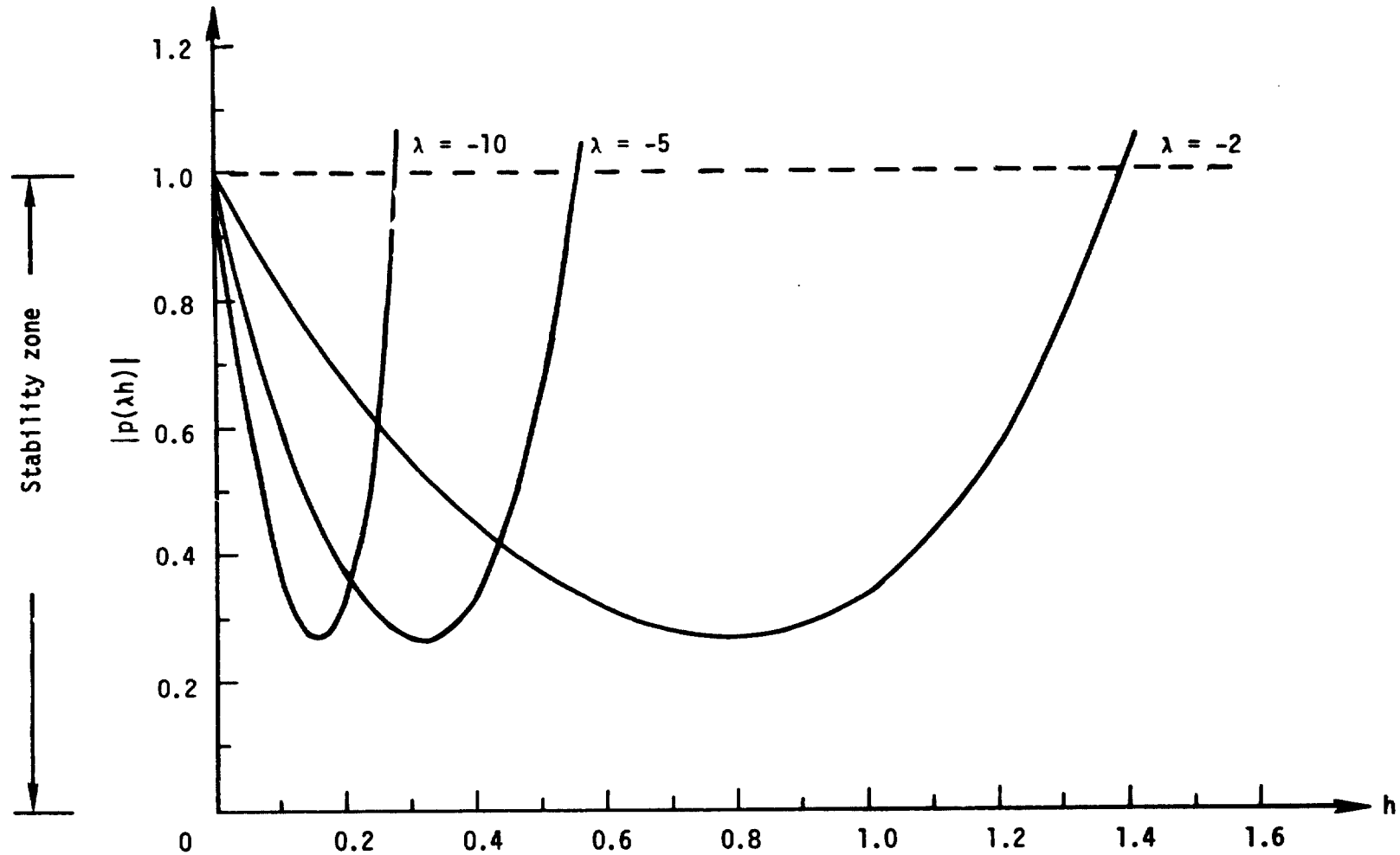


Figure 3.- Modulus of amplification factor versus step size ($\lambda$ = -2, -5, and -10).

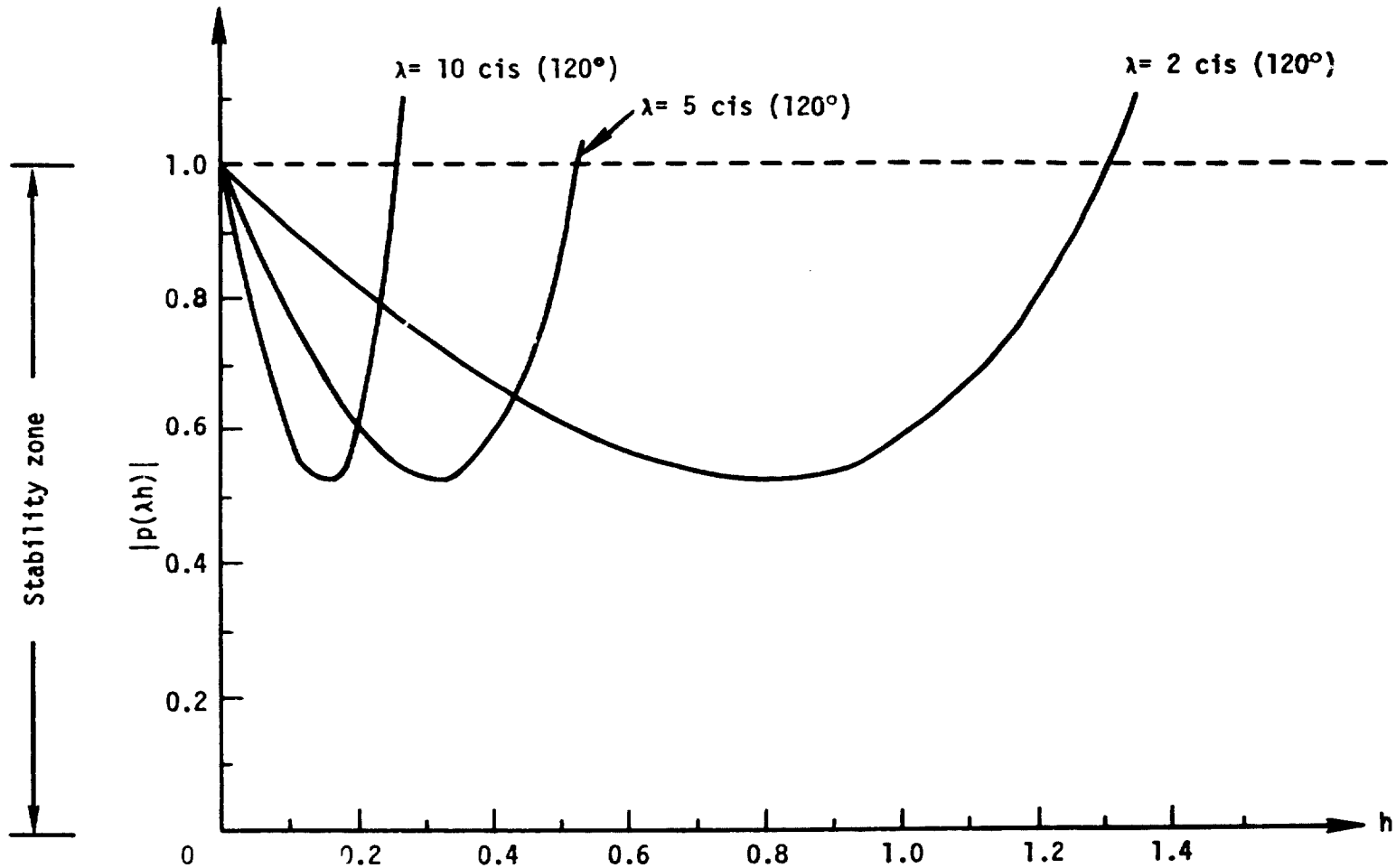


Figure 4.- Modulus of amplification factor versus step size ($\lambda = \rho(\cos 120° + i \sin 120°)$ for $\rho = 2$, 5, and 10).

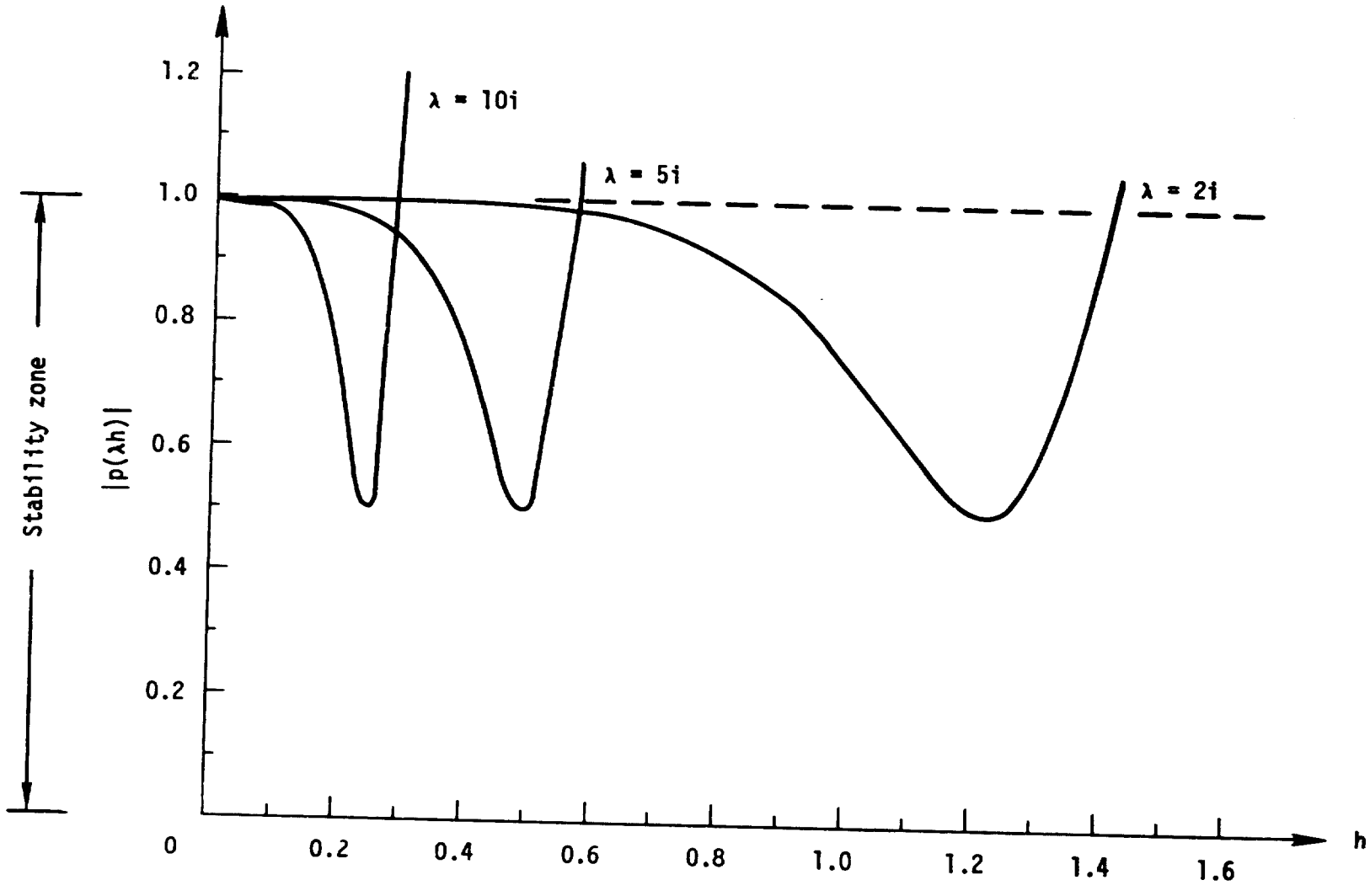


Figure 5.- Modulus of amplification factor versus step size ($\lambda = \rho i$, for $\rho$ = 2, 5, and 10 and $i^2 = -1$).

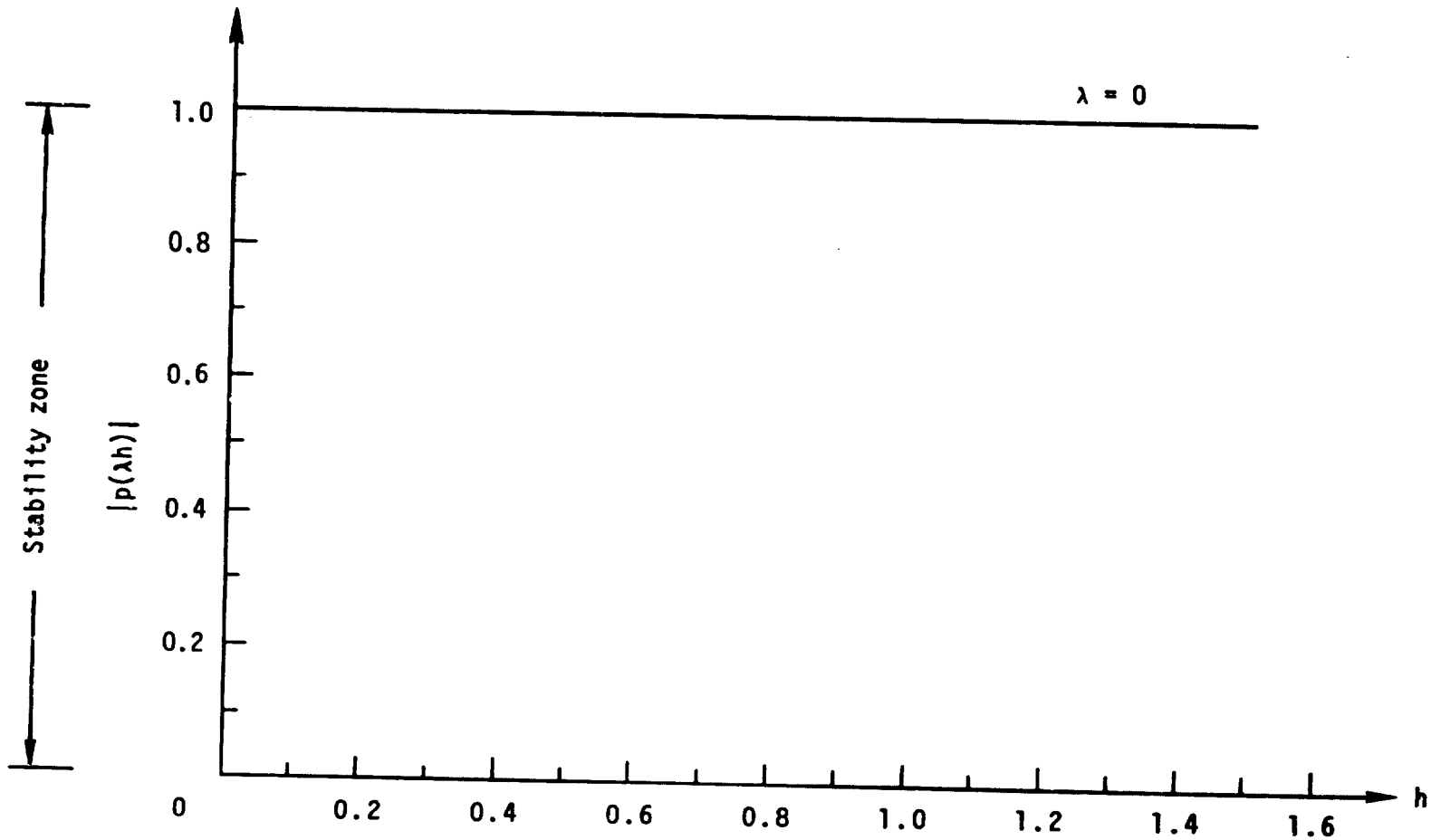


Figure 6.- Modulus of amplification factor versus step size ($\lambda = 0$).

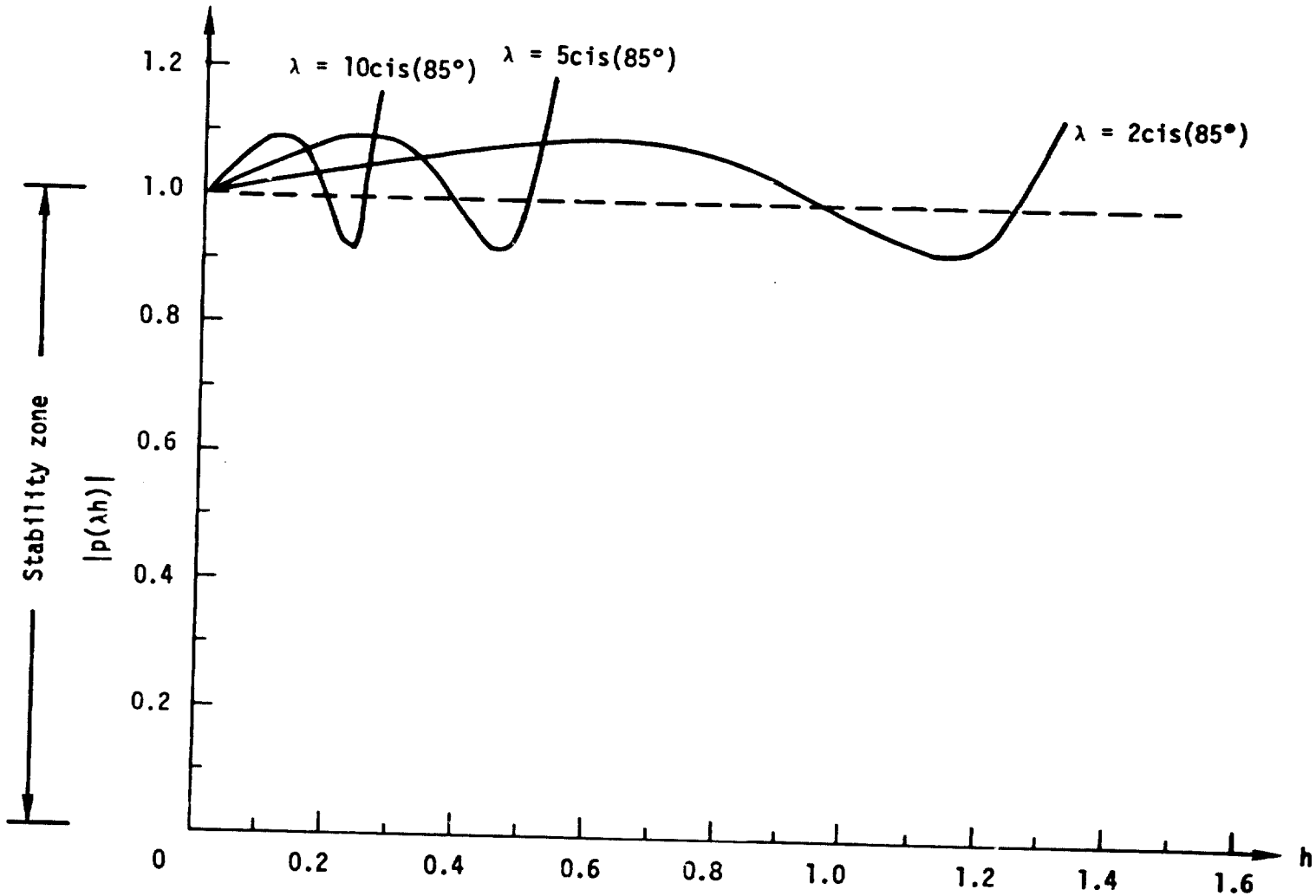


Figure 7.- Modulus of amplification factor versus step size ($\lambda = \rho(\cos 85° + i \sin 85°)$ for $\rho = 2$, 5, and 10).

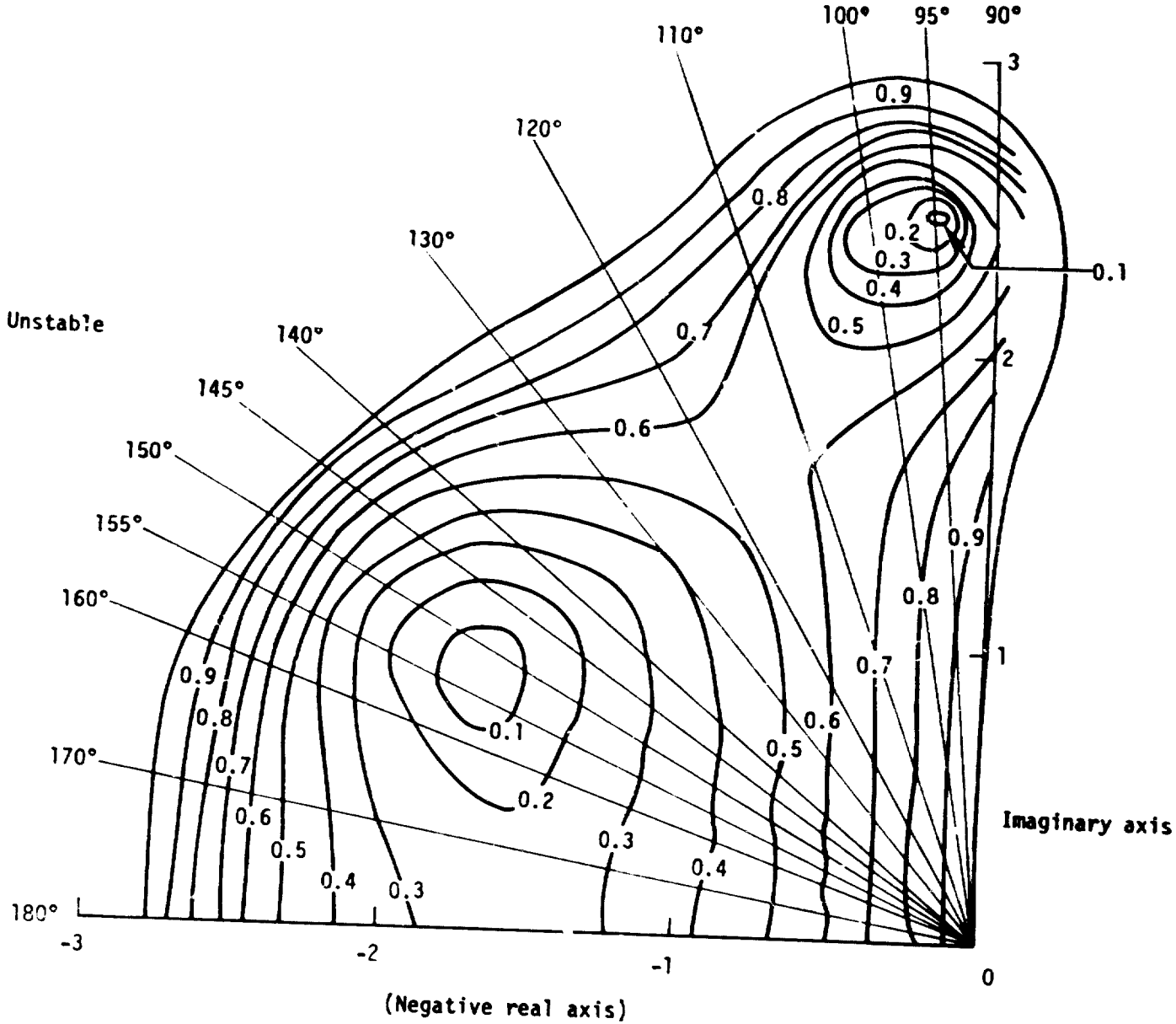


Figure 8.- Contour curves for $|p(\mu)|$ where $p(\mu)$ is the amplification factor for fourth-order Runge-Kutta method.

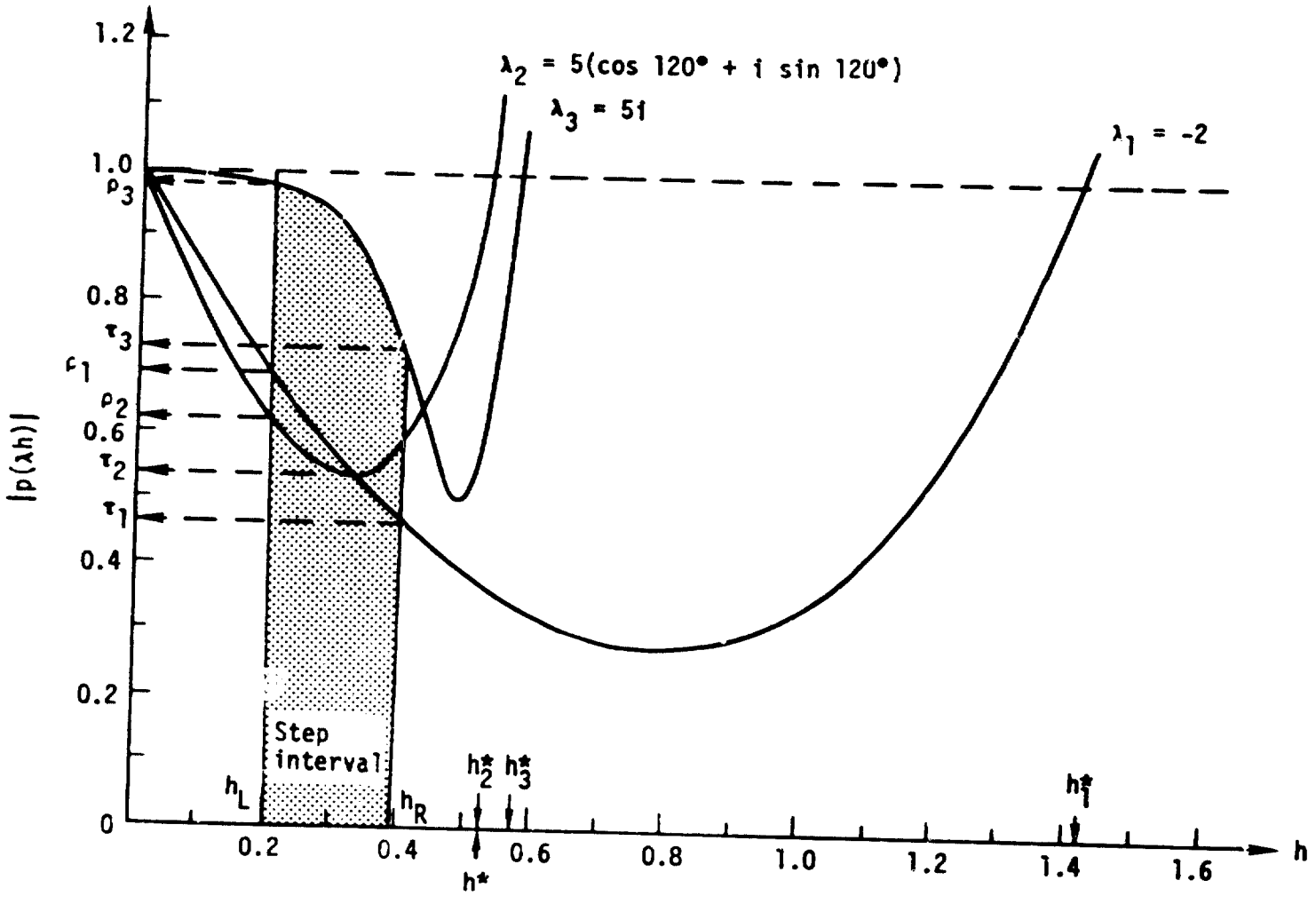


Figure 9.- Stability bounds for a specific diagonal system.

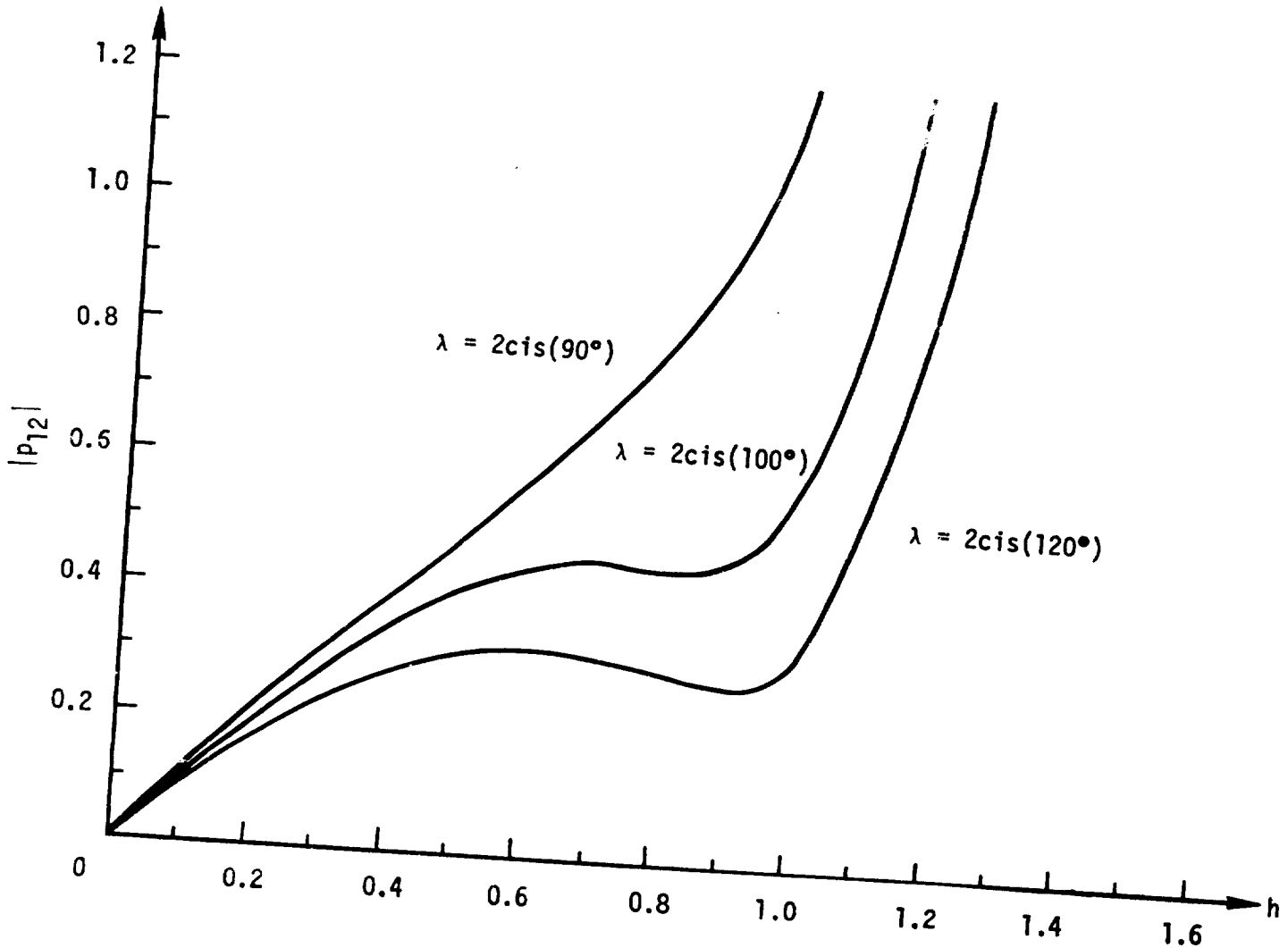


Figure 10.- Modulus of amplification factor $p_{12}$ versus step size for $\lambda = 2(\cos\theta + i \sin\theta)$ where $\theta = 90°$, 100°, ar ' 120°.

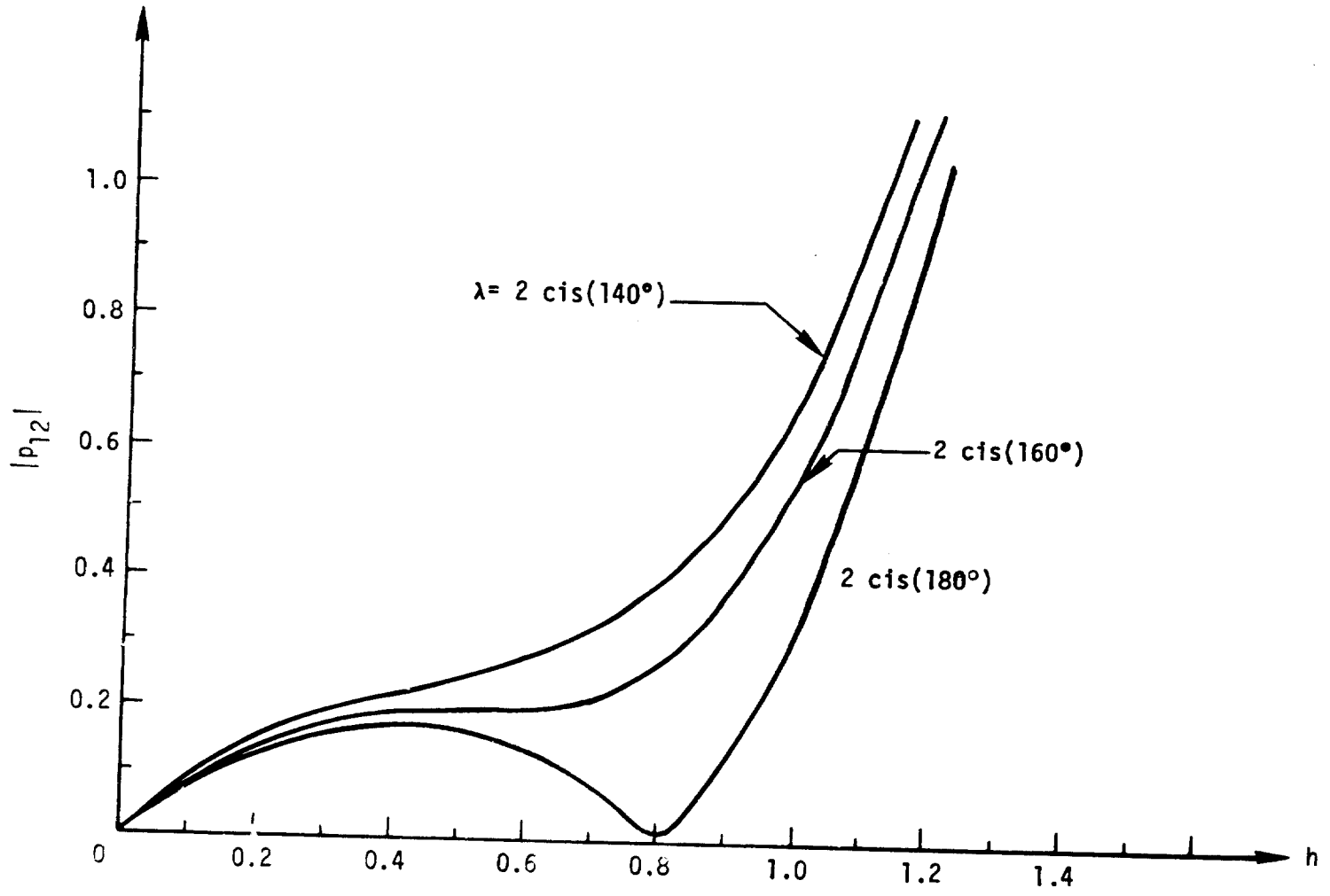


Figure 11.- Modulus of amplification factor $p_{12}$ versus step size for $\lambda = 2(\cos\theta + i \sin\theta)$ where $\theta$ = 140°, 160°, and 180°.

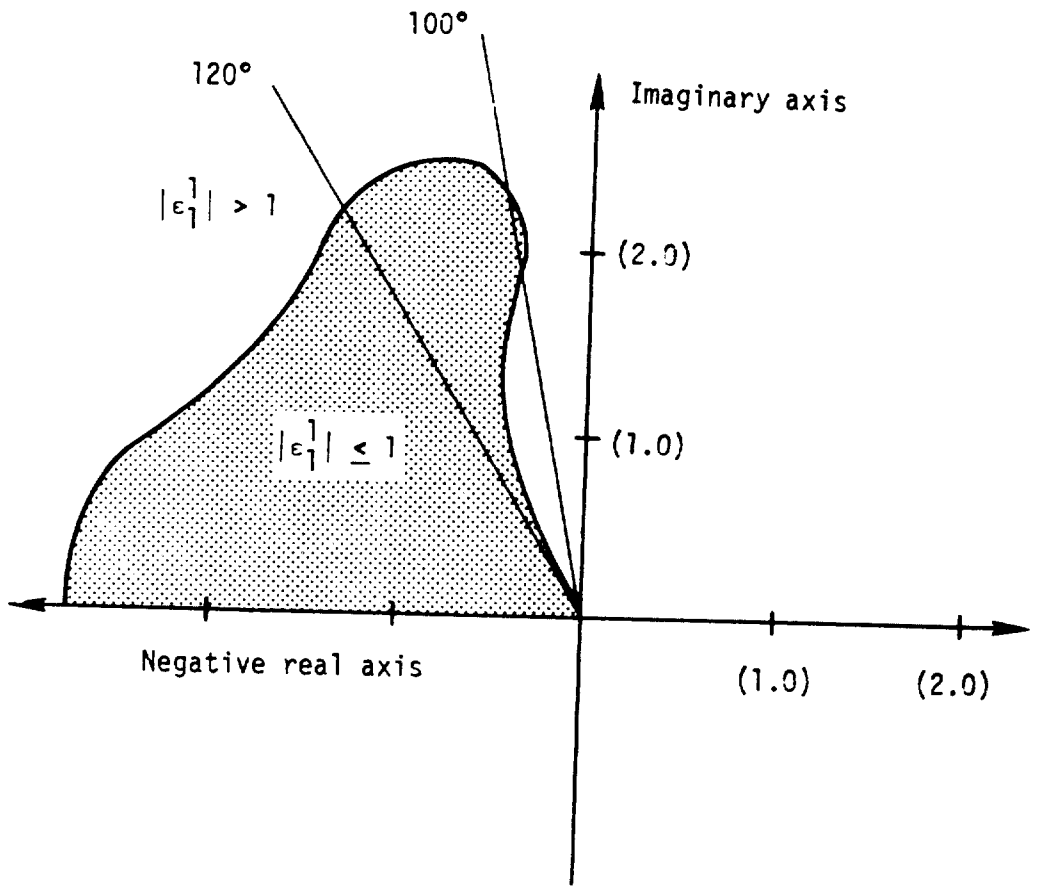


Figure 12.- One-step error propagation of $|\varepsilon_1^1|$ for $\lambda = 2(\cos\theta + i \sin\theta)$ and unit initial error.